

Thermal bridges in vacuum insulation panels at building scale

*Original*

Thermal bridges in vacuum insulation panels at building scale / Isaia, Francesco; Fantucci, Stefano; Capozzoli, Alfonso; Perino, Marco. - In: PROCEEDINGS OF THE INSTITUTION OF CIVIL ENGINEERS. ENGINEERING SUSTAINABILITY. - ISSN 1478-4629. - 170:1(2017), pp. 47-60. [10.1680/jensu.15.00057]

*Availability:*

This version is available at: 11583/2668759 since: 2017-04-06T15:02:45Z

*Publisher:*

ICE Publishing

*Published*

DOI:10.1680/jensu.15.00057

*Terms of use:*

This article is made available under terms and conditions as specified in the corresponding bibliographic description in the repository

*Publisher copyright*

(Article begins on next page)

# Thermal bridges in vacuum insulation panels at building scale

**Francesco Isaia** Eng

Research Fellow, Department of Energy, Politecnico di Torino, Turin, Italy

**Stefano Fantucci** Arch

PhD student, Department of Energy, Politecnico di Torino, Turin, Italy

**Alfonso Capozzoli** PhD

Assistant Professor, Department of Energy, Politecnico di Torino, Turin, Italy  
(corresponding author: [alfonso.capozzoli@polito.it](mailto:alfonso.capozzoli@polito.it))

**Marco Perino** PhD

Full Professor, Department of Energy, Politecnico di Torino, Turin, Italy

In this paper a numerical analysis aimed at evaluating the thermal performance of vacuum insulation panels (VIPs) at the building scale is presented. This technology has seen considerable development over the past few years, gaining increasing penetration in the building insulation market. However, it is important to evaluate correctly the thermal bridging effect that occurs when the VIPs are coupled with joints at the building scale. To this purpose, the linear thermal transmittances of different VIP assemblies inserted in several wall configurations were assessed through a bidimensional numerical analysis. Moreover, to evaluate the influence of thermal bridges on the building energy need, quasi-steady-state simulations for a parametric building module were performed. A simple empirical model was finally built to estimate the linear thermal transmittance from basic input variables. The study demonstrates that thermal bridging effects that occur when VIPs are jointed are never negligible and they could have an important impact on the building heating energy need.

## Notation

$A$	panel area
$d$	layer thickness
$l$	thermal bridge length
$P$	panel semiperimeter
$\dot{Q}$	heat flow
$R_e$	thermal resistance of outer bounding layers
$R_i$	thermal resistance of inner bounding layers
$R_i + R_e$	total thermal resistance of the bounding layers
$S$	non-adiabatic wall surface
$S/V$	aspect ratio
$V$	single-room apartment volume
$\Delta\theta$	difference between higher and lower set point temperatures
$\theta_{low}$	lower set point temperature
$\theta_{up}$	higher set point temperature
$\lambda$	thermal conductivity
$\lambda_{COP}$	vacuum insulation panel centre of panel thermal conductivity
$\lambda_{eq}$	equivalent thermal conductivity of VIP assembly
$\lambda_{eq \text{ practical}}$	VIP assembly equivalent thermal conductivity that considers thermal bridging effects in a simplified way (generally provided by VIP manufacturers)
$\lambda_{fict}$	fictitious thermal conductivity
$\psi$	linear thermal transmittance due to thermal bridge

## 1. Introduction

About 40% of overall energy consumption can be attributed to buildings (Costa *et al.*, 2013), which, in large part, are more than 20 years old (70–90% in the EU) (Bittner and Lechner, 2004). For

this reason, acting on the existing building stock is a mandatory strategy to reduce energy consumption at the global scale.

Superinsulation materials (SIMs) represent one of the most promising technologies to improve the building envelope thermal performance with the consequence of increasing the building energy efficiency. Moreover, it is possible to refurbish existing building envelopes with small thickness increments, the SIMs' thermal conductivity being five to ten times lower than that of traditional insulation materials (Johansson *et al.*, 2014a). Vacuum insulation panels (VIPs) have been studied by several researchers during the past few years, but, despite their great potential, they are still poorly adopted. This is because of the high costs, short durability (with respect to the lifetime of the building) and lack of knowledge about the thermal behaviour in real building applications, particularly relating to thermal bridging effects (Capozzoli *et al.*, 2015; Lorenzati *et al.*, 2014).

Some studies have demonstrated that the VIPs can represent a good solution for the insulation of buildings also considering sustainability aspects. In the study of Karami *et al.* (2015), a life cycle analysis was carried out by comparing a standard residential building, a well-insulated building (with traditional insulation) and a building insulated with VIPs. For the case study analysed, a lower operational primary energy and a relatively lower total greenhouse gas emission for the building insulated with VIPs were found. The study also shows that the selection of VIPs (depending on the producers) influences the environmental impact considering the industrial material production process. The investigations carried out by Ogden *et al.* (2013) promote the use

of VIPs, considering their properties to couple higher insulation performance with a relatively low embodied energy. However, in general, VIPs have a higher environmental impact in comparison with conventional insulation materials when primary energy for both production and operation is taken into account (Karami *et al.*, 2015). The investigation conducted by Schonhardt *et al.* (2003) showed that this impact can be reduced by using alternative core materials or with more energy-efficient processes for the industrial production.

‘VIP consists of a porous core enveloped by an air and vapour tight barrier which is heat sealed’ (Kalnæs and Jelle, 2014: p. 357). Many studies have been carried out on VIPs, particularly on its main components: the core material (Simmmler and Brunner, 2005) and the envelope (Wakili *et al.*, 2004). In these studies, the increase in thermal conductivity was evaluated with respect to the vacuum loss (due to gas permeation over time) and risk of damage (e.g. puncturing). In some studies the application of VIPs in new constructions or existing buildings was investigated (IEA/ECBCS, 2001; Johansson *et al.*, 2014b; Mandilaras *et al.*, 2014; Mukhopadhyaya *et al.*, 2014). Others explored possible developments of VIP technology concern new ways for fixing the panels to the other envelope layers (Boafo *et al.*, 2014, 2015) or the alternative use as internal thermal breakers (Sallée *et al.*, 2014) or innovative sandwich panels (Voellinger *et al.*, 2014).

Several investigations have focused on the thermal bridging effects related to the envelope materials (Tenpierik *et al.*, 2008), the air gaps or the structural joints between the panels and the VIP assemblies at the component or building scale (Capozzoli *et al.*, 2015; Lorenzati *et al.*, 2014). Lorenzati *et al.* (2016) carried out experimental and numerical analyses of different VIP assemblies, investigating thermal bridge effects on the geometry of the air joint between two adjacent panels, the type of structural joints and the panel size/shape. The experimental results were also used to verify a numerical model. However, the study did not explore the consequence of the thermal bridges when the VIP layer is coupled with other materials (bounding layers). Furthermore, few studies have been conducted to investigate the influence of thermal bridges on the overall building energy performance (Isaia *et al.*, 2015).

A universal conclusion from these research studies demonstrates the crucial importance of taking into account properly the thermal bridging effects to assess correctly VIP thermal performance. In fact, the higher the thermal resistance of the insulation layer, the

greater is the importance of thermal bridging effects. Even if many studies on this issue have been carried out, few investigations have been done on thermal bridging effects at the building scale, considering the VIP panels coupled with other materials and inserted in a multilayered wall (Capozzoli *et al.*, 2015; Lorenzati *et al.*, 2014).

In this paper, the thermal bridging effects of VIP panels coupled with a number of different structural joint materials or with air joints were assessed, also considering the overall multilayer structure of the wall.

The thermal conductivities of VIP panels and the structural joint materials were first evaluated through an experimental campaign. Then, the linear thermal transmittances and the equivalent thermal conductivities of different VIP assemblies (in this paper the term *assembly* is used to identify the ensemble of the VIP panels, the fixing structure and the joint) inserted in several wall configurations were calculated through a two-dimensional (2D) numerical analysis in accordance with BS EN ISO 10211:2007 (BSI, 2007a). Finally, to evaluate the influence of the VIP-related thermal bridging effect on the overall heating energy demand and transmission heat losses, several quasi-steady-state simulations were performed according to BS EN ISO 13790:2008 (BSI, 2008) for a case study.

Moreover, given the great amount of data obtained through the numerical analyses, a simple empirical model was built to estimate rapidly the linear thermal transmittance  $\psi$  on the basis of few input parameters.

## 2. Methods and methodology

### 2.1 Numerical model for the assessment of parameters to quantify the thermal bridging effects

The 2D numerical analysis was carried out through the software Physibel Bisco. The mesh was constructed using Delaunay triangulation, and then a 2D steady-state heat transfer was applied using the energy balance method. VIP panels can be found on the market with different kinds of envelopes, as well as different core materials. A metallised aluminium envelope was considered in this study, consisting of one polyethylene (PE) layer covered by three polyethylene terephthalate (PET) plus three aluminium layers (Figure 1). Some simplifications were needed to make the numerical analysis faster and more feasible, without compromising the accuracy.

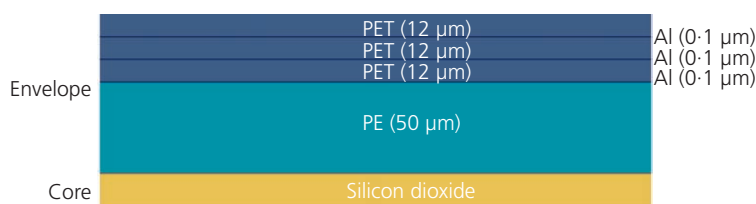


Figure 1. Metallised aluminium envelope layer

For this purpose the multilayered VIP envelope was considered through an equivalent single layer and it was modelled in the same way as by Lorenzati *et al.* (2014) and Capozzoli *et al.* (2015).

Moreover, in the model, the VIP assembly was supposed to be inserted in a multilayered wall. To analyse the effect of the additional thermal resistances, the bounding layers were modelled through a fictitious single layer on each side of the VIP panel (see top part of Figure 2). To this purpose, fictitious thermal conductivities were introduced for these simplified layers, to obtain the same thermal resistance

$$1. \quad \lambda_{\text{fict},x} = \frac{d_x}{R_x} = \frac{d_x}{\sum_{j=1}^n R_{xj}}$$

where  $R_{xj}$  are the thermal resistances of all  $j$  layers and  $d_x$  is the single fictitious layer thickness.

This procedure was done for both the exterior and the interior layers, obtaining two fictitious thermal conductivities ( $\lambda_{\text{fict}}$ ).

Heat flow and temperature values are provided as simulation output. The linear thermal transmittance was evaluated in accordance with BS EN ISO 14683:2007 (BSI, 2007b) by using the following equation

$$2. \quad \psi = \frac{\dot{Q} - (1/R_{\text{TOT}})l\Delta\theta}{\Delta\theta}$$

where

$$3. \quad R_{\text{TOT}} = R_i + R_e + \frac{d}{\lambda_{\text{COP}}}$$

Although the linear thermal transmittance of the thermal bridge  $\psi$  is a useful parameter for the detailed calculation of the heat losses, it does not allow a direct comparison between the ideal case of a homogeneous VIP insulation layer and the actual case of VIP panels jointed with other materials. For this purpose, the equivalent thermal conductivity was calculated as

$$4. \quad \lambda_{\text{eq}} = \lambda_{\text{COP}} + \psi d \left( \frac{P}{A} \right)$$

where  $\lambda_{\text{COP}}$  was measured by means of a guarded heat flux meter (GFHM) apparatus, according to UNI EN 12667:2002 (UNI, 2002).

The  $\lambda_{\text{eq}}$  depends on the panel size, in particular on the aspect ratio  $P/A$ , where  $P$  is the semiperimeter and  $A$  is the area of the panel. Therefore, a universal value of *equivalent thermal conductivity* cannot be considered. For this reason, a standard and commercially diffused panel size  $500 \times 600$  mm was considered for this analysis.

## 2.2 Parametric analysis for the evaluation of different wall configurations

The linear thermal transmittance  $\psi$  and the equivalent thermal conductivity  $\lambda_{\text{eq}}$  were assessed for different VIP assemblies inserted in several wall configurations (Isaia *et al.*, 2015).

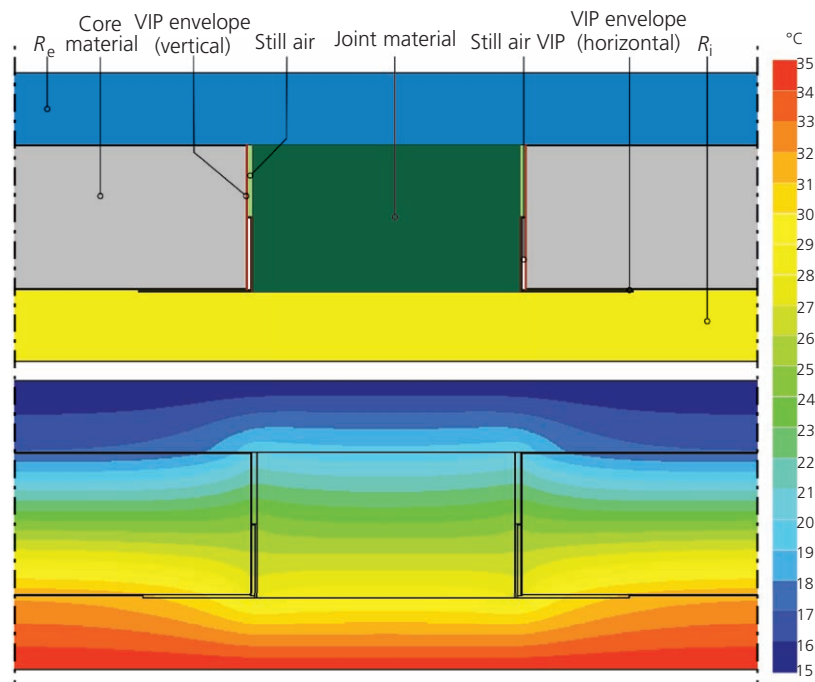


**Figure 2.** Bisco model input (top) and isothermal profile as graphical output (bottom)

To introduce the most common wall configurations, the following three wall typologies were selected in accordance with UNI-TS 11300-1:2008 (UNI, 2008)

- solid wall
- cavity wall
- insulated cavity wall.

A VIP assembly layer was then considered for each wall typology, taking into account two different solutions (interior and exterior wall insulations). In the first case, the VIP assembly was placed on the internal side of the considered wall, covered by an extra insulation layer and a drywall panel. In the second case, an exterior insulation finishing system was applied, with the VIP panels placed on the external side, followed by an extra insulation layer and plaster rendering as finishing layer.

The resulting total thermal resistances of the bounding layers is representative of realistic building envelope configurations and cover a significant range of cases.

Different ways to couple the panels were considered for both VIP configurations (interior and exterior). The case of a structural joint was analysed by considering four different materials (Isaia *et al.*, 2015), and the case of an air joint was analysed by considering three different widths of the spacer.

Regarding the structural joints, the following materials were considered: medium-density fibreboard (MDF), extruded polystyrene (XPS), rubber- and aerogel-composed blanket. To make the comparison consistent with the results from other studies available in the literature (Capozzoli *et al.*, 2015; Lorenzati *et al.*, 2014), structural joints of width 36 mm were considered.

Summarising, 24 possible combinations were analysed combining

- three wall typologies (solid wall, cavity wall and insulated cavity wall)
- two insulation configurations (interior and exterior)
- four possible extra insulation layers (0, 20, 40 or 60 mm thick) characterised by a thermal conductivity  $\lambda = 0.035 \text{ W/(m K)}$ .

For each wall configuration, three different VIP thicknesses were considered (10, 20 or 30 mm) combined with seven possible joint materials/typologies (in particular, four different materials for

structural joint and three different widths of air gap for the air joint), resulting in 504 wall structures (Figure 3).

### 2.3 Numerical model for the assessment of building energy performance

A residential building presented by Isaia *et al.* (2015) was selected as a case study, and the energy performance was evaluated taking into account all the wall configurations described above. The building geometrical model is shown in Figure 4, and the boundary conditions for the simulations are shown in Table 1.

To take different aspect ratios into account, the building energy performance analyses were performed considering the following four different configurations (Figure 4)

- all external walls
- one adiabatic wall
- two adiabatic walls
- three adiabatic walls.

The floor and the ceiling in the analysed case study were assumed to be adiabatic because the thermal bridging effects associated with VIP assemblies were evaluated considering exclusively different configurations of vertical walls.

The analyses were carried out considering three different thermal conductivity values of the VIP assembly's layer inserted in each wall configuration.

## 3. Results and discussion

Three different values for the thermal conductivity of the VIP assembly layer were considered for the evaluation of the building's transmission heat losses and heating energy need

- the equivalent thermal conductivity,  $\lambda_{eq}$ , to take into account the thermal bridging effects in a rigorous way, based on the 2D numerical analyses (evaluated with Equation 4 and a  $500 \times 600 \text{ mm}$  panel)
- the practical equivalent thermal conductivity,  $\lambda_{eq,practical} = 0.007 \text{ W/(m K)}$ , to take into account the thermal bridging effects in a simplified way by incrementing the centre of panel thermal conductivity (this value does not take into account the VIP panel shape/size)
- the centre of panel thermal conductivity,  $\lambda_{COP}$ , to evaluate indirectly the weight of the thermal bridging effect (since this represent the ideal best scenario).



Figure 3. Different combinations of wall configurations

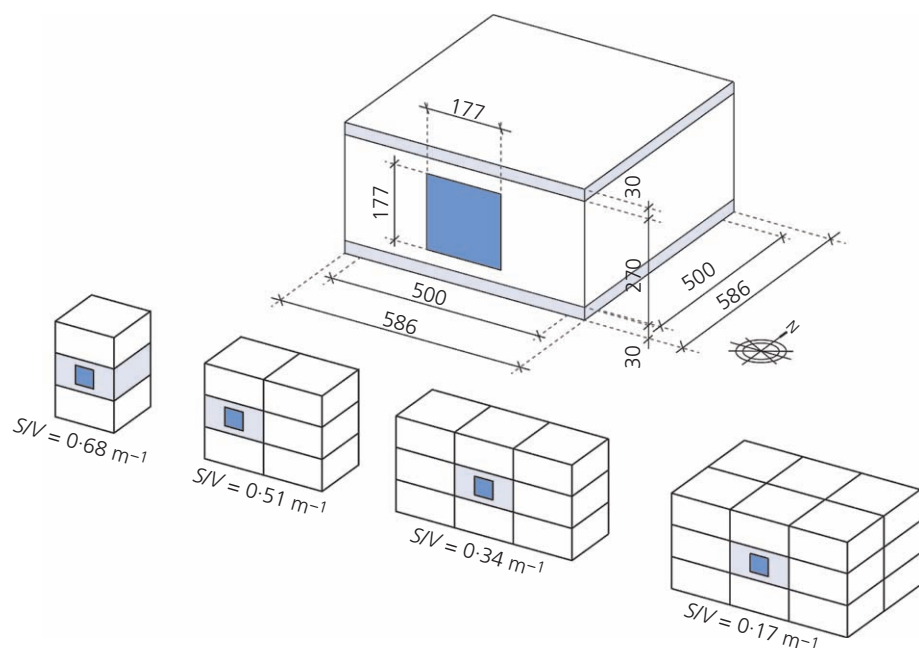


**Figure 4.** Three-dimensional model of the building case (units of measurement: cm)

The following outcomes were chosen to evaluate the building energy performance, in accordance with BS EN ISO 13790:2008 (BSI, 2008)

- $H_{tr}$ : heat transfer coefficient by transmission
- $Q_H$ : building heating energy demand.

In this way, the results made it possible to evaluate the influence of the thermal bridging effects related to the VIP assembly on the

Boundary condition	Value
Location	Torino
Heating degree day	2617 (BS EN ISO 14683:2007)
Heating period	15 October–15 April
Internal temperature	20°C (293.15 K)
Internal dimensions	5 × 5 × 2.7 m
Window dimensions	1/8 plan area, minimum for natural light and ventilation according to the Italian law (Italian Ministry of Health, 1975) (Figure 4)
Window thermal transmittance	$U_w = 2 \text{ W/m}^2 \text{ K}$
Ventilation	Only infiltration ( $0.3 \text{ h}^{-1}$ )
Floor and ceiling	Adiabatic
Wall transmittance	Variable ( $U_{eq} = 0.106 \div 0.470 \text{ W/m}^2 \text{ K}$ )
Internal heat gain	$4.90 \text{ W/m}^2$

**Table 1.** Boundary conditions of the building case study

building energy performance. To isolate the thermal bridging effect due to VIPs on the building energy performance, no other kinds of thermal bridges were considered in the model (e.g. due to the structure or to geometrical nodes or discontinuities).

**3.1 Evaluation of linear thermal transmittance and equivalent thermal conductivity**

The centre of panel thermal conductivities assessed through the experimental campaign are shown in Table 2 for the VIPs and structural joints. The thermal conductivity of the aerogel blanket was assumed equal to the mean value of a manufacturer’s declaration (for this reason the uncertainty is not specified) (Aspen Aerogels, Inc., 2015).

The equivalent thermal conductivity of the air gap between two panels (air joint VIP assembly) used in the model was evaluated

Joint material	$\lambda$ : W/m K
VIP 10 mm	$0.0054 \pm 0.0001$
VIP 20 mm	$0.0046 \pm 0.0001$
VIP 30 mm	$0.0048 \pm 0.0001$
MDF	$0.1034 \pm 0.0021$
XPS	$0.0350 \pm 0.0007$
Rubber	$0.2053 \pm 0.0042$
Aerogel	0.015

**Table 2.** Centre of panel thermal conductivities assessed through the experimental campaign



according to the BS EN ISO 6946:2007 guidelines (simplified calculation method) (BSI, 2007c) following the procedure adopted by Lorenzati *et al.* (2016).

Therefore, a parametric analysis was first carried out for three joint widths and three panel thicknesses. In Figure 5 the variation in the linear thermal transmittance as a function of the total thermal resistance is shown considering different widths of spacer and a 20-mm VIP. By analysing the effect of the thermal bridge, it is possible to see (Figure 5) that the linear thermal transmittance decreases when the size of the air joint becomes smaller and when the total thermal resistance increases.

To compare the VIP assembly with air and structural joints, in the successive analyses only one width of spacer is considered. In particular, a 3.5-mm width of air joint between the panels was selected according to Lorenzati *et al.* (2016). This width can be considered as an average value commonly adopted in real building applications.

The variation in the linear thermal transmittance as a function of the total thermal resistance of the bounding layers ( $R_i + R_e$ ) is shown in Figures 6, 7 and 8 for 30-, 20- and 10-mm VIP, respectively.

From an analysis of the figure, it is clear that the linear thermal transmittance decreases with increase in  $R_i + R_e$  and tends to converge to a narrow range.

To have an idea of the effects of the various joint configurations on the performance of realistic wall structures to be used for typical building renovations and/or constructions, two multilayered components were considered.

For  $R_i + R_e = 1 \text{ m}^2 \text{ K/W}$  (dashed vertical line in Figure 6), which represents the additional thermal resistance of a rough cavity wall, the  $\psi$  value ranges from  $\sim 0.011$  (air joint of 3.5 mm) to  $\sim 0.038 \text{ W/(m K)}$  (rubber joint).

Moreover, for  $R_i + R_e = 2 \text{ m}^2 \text{ K/W}$  (dotted vertical line in Figure 6), which represents the additional thermal resistance of a cavity wall with 40 mm of extra insulation layer, the  $\psi$  value is almost halved compared with that of the previous case and goes from  $\sim 0.006$  (air joint of 3.5 mm) to  $\sim 0.019 \text{ W/(m K)}$  (rubber joint).

As expected, the lowest values of  $\psi$  are reached for a simple air joint between adjacent VIPs; nevertheless, similar results are obtained with a structural joint made of aerogel. Using aerogel – a material that performs very well in terms of thermal properties – is almost as good as having a 3.5-mm air joint.

Figures 7 and 8 show a trend analogous to that in Figure 6. For the analysed configurations, the linear thermal transmittance values slightly decrease with the VIP thickness, demonstrating that thicker VIPs are more influenced by thermal bridging effects, particularly when the thermal resistance of the bounding layers becomes higher. This behaviour demonstrates that the higher the value of  $R_i + R_e$  is, the lower is the entity of the thermal bridge.

A relevant outcome from these results shows that highly insulating structural joints (XPS or aerogel-based joints) represent suitable materials for assembling VIPs during the application phase. VIP coupling materials are of key importance, since they are used in a range of applications (e.g. in laths, battens, corners and to cover discontinuities).

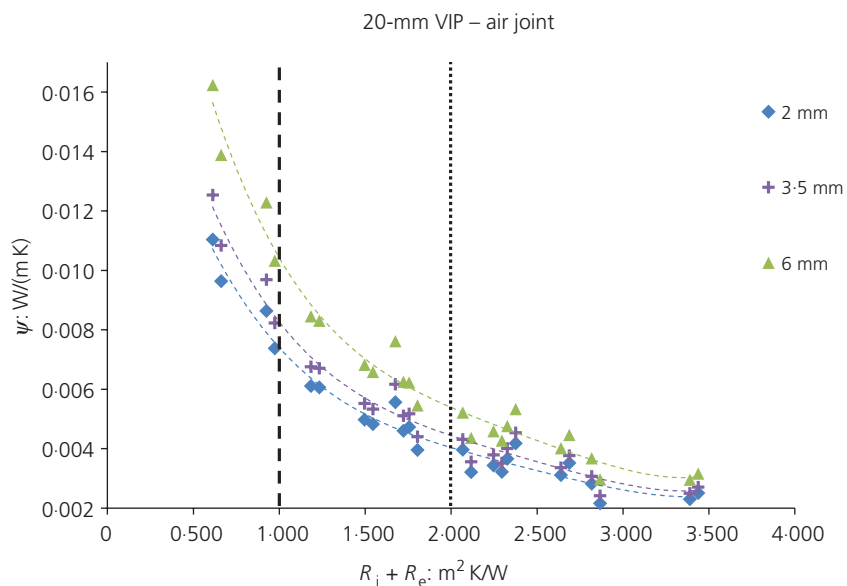


**Figure 5.** Linear thermal transmittances ( $\psi$ ) as a function of total thermal resistance (20-mm VIP) for different widths of air joint

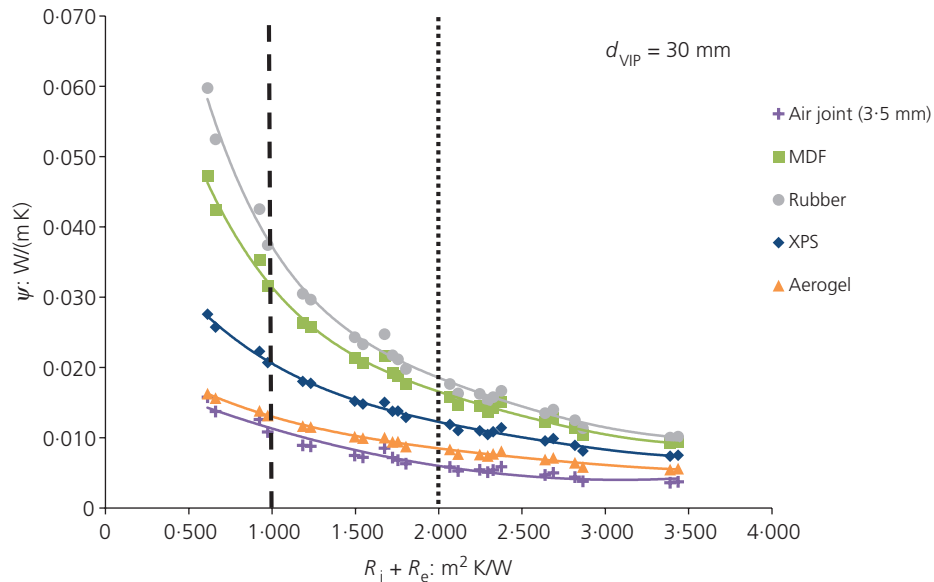


**Figure 6.** Linear thermal transmittances ( $\psi$ ) as a function of total thermal resistance (30-mm VIP)

To consider further the impact of thermal bridging effects, the percentage difference between  $\lambda_{eq}$  and  $\lambda_{COP}$  for a  $500 \times 600$  mm VIP panel was calculated and is plotted in Figure 9 as a function of  $R_i + R_e$ .

- For  $R_i + R_e = 1 \text{ m}^2 \text{ K/W}$  (dashed vertical line), the percentage differences between  $\lambda_{eq}$  and  $\lambda_{COP}$  range from ~5% (air joint with a 10-mm VIP) to ~72% (MDF joint with 30-mm VIP).

- For  $R_i + R_e = 2 \text{ m}^2 \text{ K/W}$  (dotted vertical line), values ranging from ~2% to ~38% were found.

These results are in line with those reported for the  $\psi$  values and indicates that the higher the thermal resistance of the bounding layers is, the lower is the increment of  $\lambda_{eq}$  in comparison with the  $\lambda_{COP}$ .

The curves in Figure 9 are divided into three groups. Fixing the joint material, the 30-mm VIP curves (solid lines) are located on

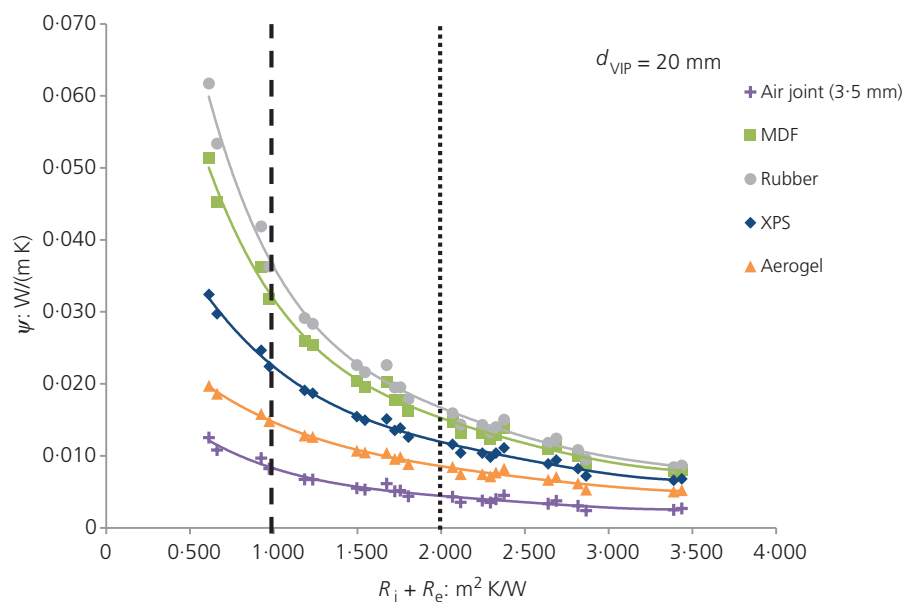


**Figure 7.** Linear thermal transmittances ( $\psi$ ) as a function of total thermal resistance (20-mm VIP)



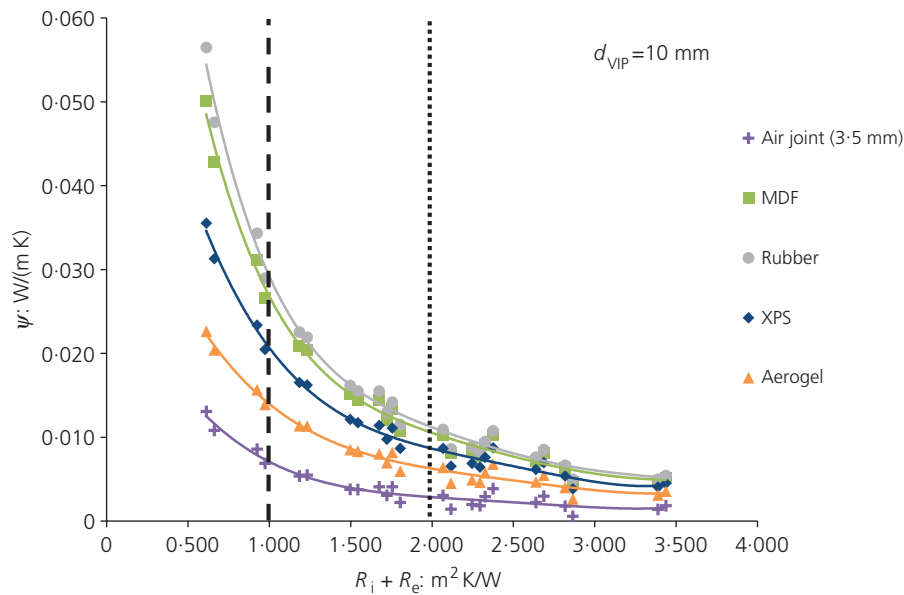


**Figure 8.** Linear thermal transmittances ( $\psi$ ) as a function of total thermal resistance (10-mm VIP)

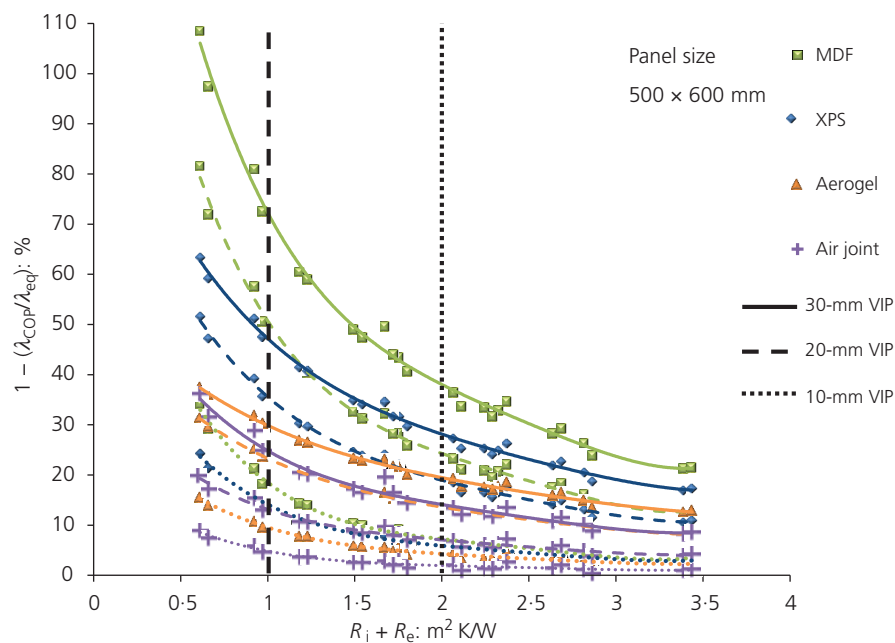


**Figure 9.** Percentage difference between  $\lambda_{eq}$  and  $\lambda_{COP}$  as a function of total thermal resistance

the upper part; the 20-mm VIP curves (dashed lines), in the middle; and the 10-mm VIP (dotted lines), at the bottom.

Another important consideration is that the increase in the VIP thickness corresponds to an increase in the percentage difference between  $\lambda_{eq}$  and  $\lambda_{COP}$ , and the increment between the minimum

and the maximum values of the percentage difference is more evident for thicker VIPs.

Considering the XPS joint, the variation between the lowest  $R_i + R_e$  ( $0.612 \text{ m}^2 \text{ K/W}$ ) and the highest  $R_i + R_e$  ( $3.437 \text{ m}^2 \text{ K/W}$ ) values are  $\sim 46$ ,  $\sim 40$  and  $\sim 21\%$  for 30-, 20- and 10-mm VIPs,

respectively. Analogous results can be found considering the range of percentage differences between the 10- and the 30-mm-thick panels, considering the MDF joints. This range is  $\sim 74\%$  for the lowest  $R_i + R_e$  value and  $\sim 17\%$  for the highest one.

### 3.2 Building energy performance evaluation

The building energy performance of the case study previously described was assessed for all the wall typologies and VIP assemblies investigated in the parametric analysis.

The analyses were aimed at examining the differences in the building energy performance considering three values of thermal conductivity of the VIP assembly ( $\lambda_{COP}$ ,  $\lambda_{eq}$  and  $\lambda_{eq,practical}$ ) inserted in the multilayered structure of the wall. The results are related to the boundary conditions assumed for the case study (see Table 1). However, the difference between the cases can be considered consistent and useful for obtaining general trends and extracting general considerations on the thermal bridging effects.

In Figure 10 the building heating energy need  $Q_H$  per square metre (normalised on net floor area) is plotted against the building aspect ratio ( $S/V$ ). In particular, the variation in building heating energy need is shown only for a certain total thermal resistance of the bounding layers (internal insulation in a solid wall with 20 mm of additional insulation material) considering different joint solutions and three different VIP thicknesses. Moreover, a reference curve is plotted (COP) for each VIP thickness. In this case the centre of panel thermal conductivity was set for the VIP layer (absence of thermal bridging effects).

It is clear that the coupling joint material does not affect significantly the building heating energy need in the case of the 10-mm-thick VIP (see continuous lines on the upper part of

the graph in Figure 10). When considering 20- and 30-mm VIP, however, the influence of joint materials on the building heating energy need is more evident. According to these conclusions, the higher the VIP thickness is (and consequently its thermal resistance), the higher is the influence of thermal bridging effects on the heating energy need.

The percentage differences between  $H_{tr}$  (heat transfer coefficient by transmission) calculated considering  $\lambda_{COP}$  or  $\lambda_{eq,practical}$  instead of  $\lambda_{eq}$  were also evaluated to investigate the influence of the thermal bridging effects on this parameter. This analysis was performed considering 20-mm-thick VIP, XPS and air joints and different aspect ratios (Figures 11 and 12).

Figure 11 shows the percentage difference between  $H_{tr}$  (heat transfer coefficient by transmission) calculated, assuming for the VIP assembly first  $\lambda_{COP}$  and then  $\lambda_{eq}$ . This analysis is shown for 20-mm VIPs coupled with the XPS joint and with an air joint (air gap 3.5-mm width). The building envelope heat transfer coefficient calculated considering the equivalent thermal conductivity is higher because it takes into account the thermal bridging effects. The percentage difference increases with the decrease in the total thermal resistance of the bounding layers ( $R_i + R_e$ ) and with the increase in the aspect ratio. Considering the XPS joint, this difference reaches up to 27% for an aspect ratio of 0.68 and the lowest value of total thermal resistance of the bounding layers.

Even though the percentage differences reach low values for high  $R_i + R_e$  values, the effect of thermal bridging effects can never be considered negligible.

In Figure 12 the heat transfer coefficient by transmission was calculated considering a practical equivalent thermal conductivity,

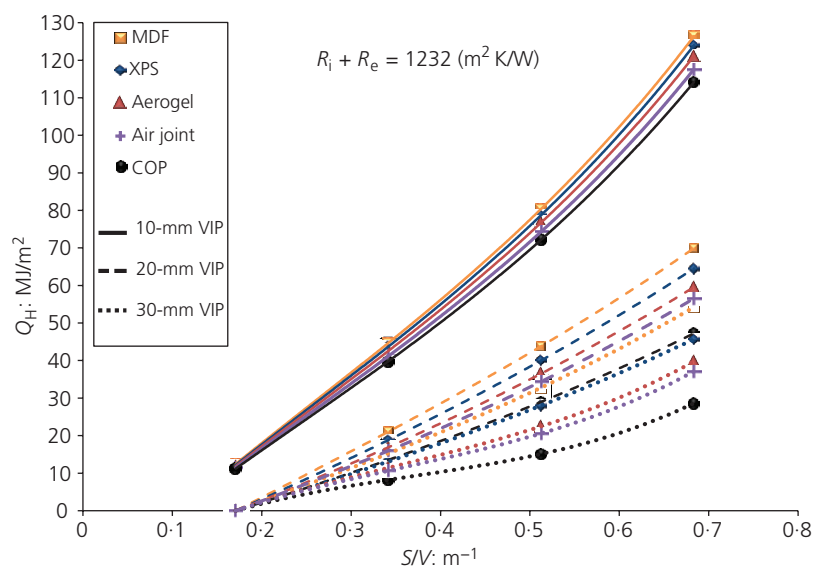


**Figure 10.** Building heating energy need variation for different VIP thicknesses and different surface-to-volume ratio,  $S/V$

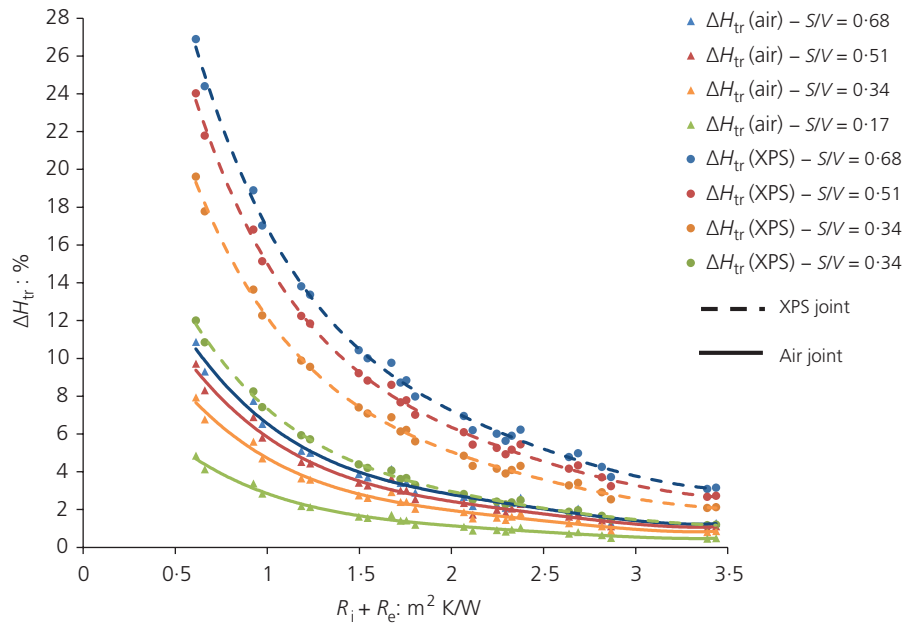


**Figure 11.** Percentage difference between  $H_{tr}$  calculated with  $\lambda_{eq}$  and  $\lambda_{COP}$  – XPS joint

$\lambda_{eq}$  practical, instead of  $\lambda_{eq}$  for the VIP assembly. In this case, the percentage differences are always negative because  $\lambda_{eq}$  practical is always higher than  $\lambda_{eq}$ . This means that by using a practical equivalent thermal conductivity, an underestimation of VIP thermal performance occurs. The percentage differences reach no negligible absolute values, as in the previous case.

From the analyses it can be inferred that the thermal bridging effects in VIPs strongly affect the heat transfer coefficient by transmission  $H_{tr}$ . Excluding the rubber joint case, the percentage differences can reach values of up to 51% in the case of external insulation in a solid wall using 30-mm VIP coupled with MDF joints (this case is not shown in the previous figures for the sake of brevity).

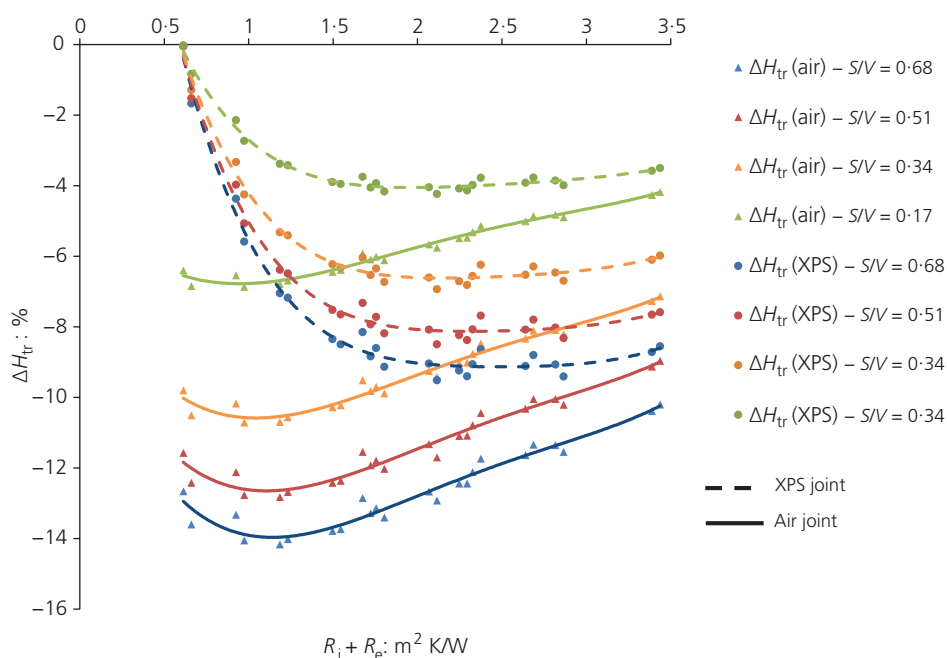


**Figure 12.** Percentage difference between  $H_{tr}$  calculated with  $\lambda_{eq}$  and  $\lambda_{eq}$  practical – XPS joint

	10-mm VIP		20-mm VIP		30-mm VIP	
	$\alpha_1$	$\alpha_2$	$\alpha_1$	$\alpha_2$	$\alpha_1$	$\alpha_2$
$\beta_1$	$-1.06 \times 10^{-3}$	$4.20 \times 10^{-4}$	$-1.04 \times 10^{-3}$	$5.01 \times 10^{-4}$	$-1.04 \times 10^{-3}$	$9.20 \times 10^{-4}$
$\beta_2$	$1.01 \times 10^{-2}$	$-4.55 \times 10^{-3}$	$9.98 \times 10^{-3}$	$-5.12 \times 10^{-3}$	$9.98 \times 10^{-3}$	$-9.16 \times 10^{-3}$
$\beta_3$	$-3.56 \times 10^{-2}$	$1.89 \times 10^{-2}$	$-3.58 \times 10^{-2}$	$2.03 \times 10^{-2}$	$-3.58 \times 10^{-2}$	$3.48 \times 10^{-2}$
$\beta_4$	$5.59 \times 10^{-2}$	$-3.77 \times 10^{-2}$	$5.83 \times 10^{-2}$	$-4.03 \times 10^{-2}$	$5.83 \times 10^{-2}$	$-6.39 \times 10^{-2}$
$\beta_5$	$-3.53 \times 10^{-2}$	$3.52 \times 10^{-2}$	$-3.99 \times 10^{-2}$	$4.20 \times 10^{-2}$	$-3.99 \times 10^{-2}$	$5.82 \times 10^{-2}$

**Table 3.** Coefficients of the logarithmic equation

#### 4. Construction of a simple empirical model

The high amount of data generated through the numerical simulations suggested the evaluation of the possibility of building a simple empirical model for the estimation of the linear thermal transmittance values ( $\psi$ ). Such a model can allow a fast and easy evaluation of a key design parameter on the basis of the total thermal resistance of the bounding layers ( $R_i + R_e$ ) and the thermal resistance of joint material, assuming the VIP typology (centre of panel thermal conductivity, core and envelope features) and three different thicknesses analysed in this paper.

The aim was methodological, to verify the practical application of this procedure. If the use of a simple empirical model is found to be profitable, this approach should be extended. For each kind of panel and configuration, detailed simulations will have to be performed by varying all the influencing parameters (with a procedure similar to that used to create the atlas for the thermal bridges).

To build the empirical model relative to structural joints, the data set, consisting of 288 different cases, was splitted into two parts: a training and a testing sub-data set. In particular, about 70% of cases were selected randomly and uniformly through the whole data set for the construction of the empirical model. The remaining 30% of the data set were used for testing the model.

The model was built considering the linear thermal transmittance variation with the total thermal resistance of the bounding layers. The results for all the structural joints are analysed for a given VIP thickness (30, 20 and 10 mm). Each data set was fit by using a fourth-grade polynomial curve.

For each of the three VIP thickness and for each joint, a polynomial function was found

$$\psi_k = \beta_{1j,k}(R_i + R_e)^4 + \beta_{2j,k}(R_i + R_e)^3 + \beta_{3j,k}(R_i + R_e)^2 + \beta_{4j,k}(R_i + R_e) + \beta_{5j,k}$$

where  $\beta_{j,k}(1 \leq j \leq 4; 1 \leq k \leq 3)$  are the coefficients of the polynomial equation. Each  $j$  refers to each joint material, and  $k$  is related to each VIP thickness.

Four polynomial functions (one for each joint) were evaluated for each VIP thickness. Twenty coefficients, one for each VIP thickness, were evaluated.

To make the model useful for a wider set of different structural joint cases, a logarithmic interpolation of the previously described coefficients was performed with respect to the joint thermal resistance

$$6. \quad \beta_{n,j,k}(1 \leq n \leq 5) = \alpha_{1k,n} \ln(R_{\text{joint}}) + \alpha_{2k,n}$$

For each VIP thickness, five functions were evaluated, one for each coefficient  $\beta_{j,k}$ . The ten coefficients  $\alpha$  found for each VIP thickness are reported in Table 3.

In this way, for a given VIP thickness, it is possible to evaluate the linear thermal transmittance, having as inputs the joint thermal resistance and the total thermal resistance of the bounding layers. Three spreadsheets (one for each VIP thickness) can be implemented to evaluate immediately the linear thermal transmittance starting from the previously described inputs.

Equation 5 can be rewritten by including Equation 6, thus having a complete form of the empirical model

$$\begin{aligned} \psi_k = & [\alpha_{1k,1} \ln(R_{\text{joint}}) + \alpha_{2k,1}](R_i + R_e)^4 \\ & + [\alpha_{1k,2} \ln(R_{\text{joint}}) + \alpha_{2k,2}](R_i + R_e)^3 \\ & + [\alpha_{1k,3} \ln(R_{\text{joint}}) + \alpha_{2k,3}](R_i + R_e)^2 \\ & + [\alpha_{1k,4} \ln(R_{\text{joint}}) + \alpha_{2k,4}](R_i + R_e) \\ 7. & + [\alpha_{1k,5} \ln(R_{\text{joint}}) + \alpha_{2k,5}] \end{aligned}$$

To evaluate the entity of the errors in using this model instead of performing numerical analyses, the linear thermal transmittances (included in the testing data set) assessed through the software Physibel Bisco ( $\psi$ ) were calculated with the model ( $\psi_{\text{model}}$ ), starting from the same inputs. The result was plotted, having the identity line as the optimum case (Figure 13). Moreover, the coefficient of determination ( $R^2$ ) and the mean absolute percentage error ( $E_{\text{MAP}}$ ) were calculated to estimate the empirical

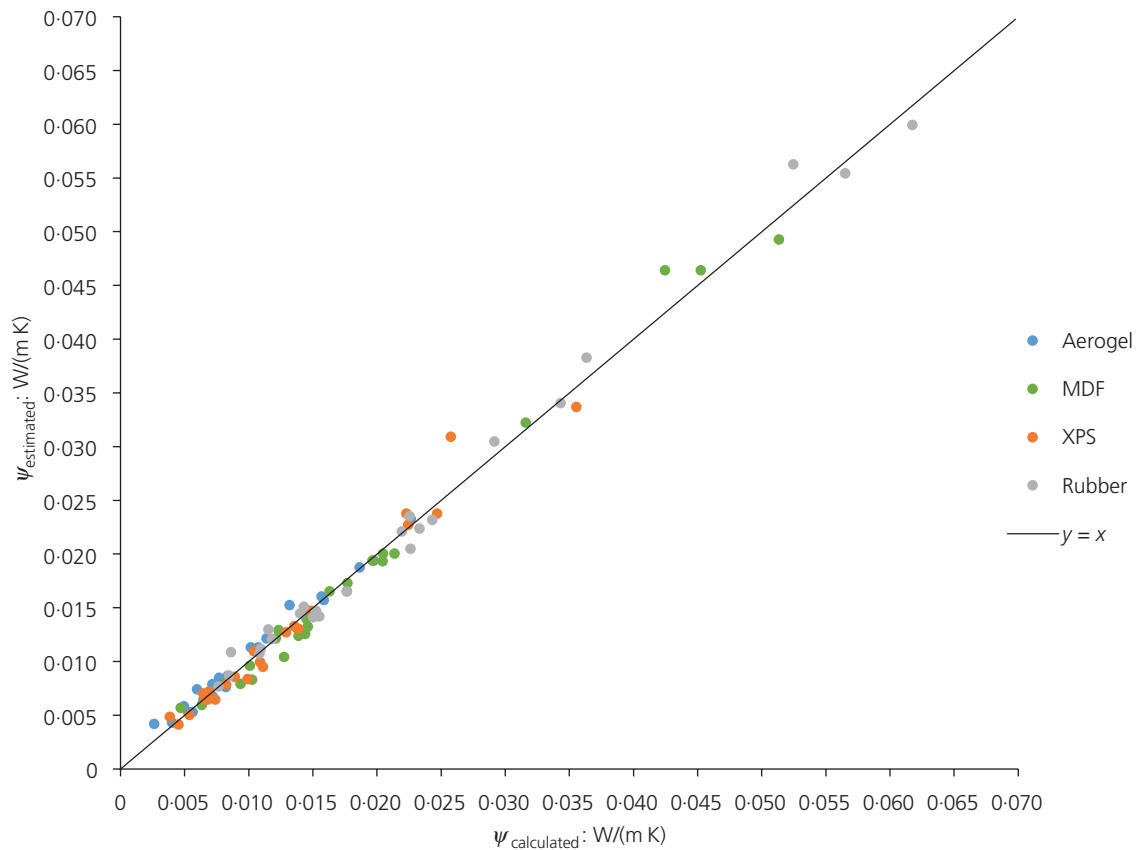


**Figure 13.** Linear thermal transmittance estimated with the empirical model and calculated with 2D numerical analysis

model performance, and they were found to be 0.989 and 2.39%, respectively. The  $E_{\text{MAP}}$  value was calculated through the following equation

$$8. \quad E_{\text{MAP}}(N) = \frac{1}{N} \sum_{i=1}^n \left| \frac{y_i - \hat{y}_i}{y_i} \right| 100$$

where  $y_i$  is the calculated linear thermal transmittance with the numerical model,  $\hat{y}_i$  is the estimated linear thermal transmittance and  $N$  is the sample size.

In the case of the air joint (3.5 mm), the empirical equation assumes the same form of Equation 5. The only difference is that

in this case  $j = 1$ , since only one width of spacer was considered. The  $\beta$  coefficients relative to the air joint are reported in Table 4.

As mentioned, this study was mainly aimed at evaluating the methodological approach, as the simulations were performed for a unique VIP typology (in terms of core and envelope technologies and centre of panel thermal conductivity) considering a limited range of thicknesses, the empirical model has some limitations. However, the range of total thermal resistances of the bounding layers and thermal resistances of structural joints cover a significant number of realistic cases.

Clearly, to have a higher practical impact, this kind of procedure should be repeated for different VIP types.

3.5-mm air joint	$\beta_1$	$\beta_2$	$\beta_3$	$\beta_4$	$\beta_5$
10-mm VIP	0.000722	−0.007119	0.026156	−0.043684	0.030990
20-mm VIP	0.000450	−0.004371	0.016087	−0.028224	0.024319
30-mm VIP	0.000502	−0.004875	0.017967	−0.031973	0.029188

**Table 4.** Air joint coefficients

## 5. Conclusions

VIPs are a promising technology that can contribute significantly to the energy demand reduction in the building sector. In particular, it could be crucial in the energy refurbishment of existing building stock and in new high-performance building elements. The thermal properties of this technology make it possible to obtain high insulated building envelopes with low thickness.

However, different drawbacks interfere with the diffusion of this technology. To inhibit the VIP diffusion, there are, on the one hand, high costs and uncertain durability (compared with the lifetime of a building); on the other hand, there are difficulties in evaluating the panels' thermal behaviour and in assessing their overall thermal performance in real applications. For the first issue, a cost reduction is expected in the future. Moreover, the space saving by adopting VIPs instead of traditional insulation materials can neutralise the initial investment costs. The second issue needs to be tackled scientifically, adopting new testing methods to evaluate correctly the VIP thermal properties (Lorenzati *et al.*, 2015, 2016) and providing simplified methodologies to assess the thermal performance of a VIP assembly inserted in a wall configuration.

In this paper the linear thermal transmittances and the equivalent thermal conductivities of VIPs assembled with different joint materials/typologies inserted in several wall configurations were evaluated through a 2D numerical analysis. Then, to evaluate the influence of the VIP-related thermal bridging effect on the overall building heating energy need, several quasi-steady-state simulations were performed according to BS EN ISO 13790:2008 (BSI, 2008) for a case study.

The results have demonstrated that the linear thermal transmittance values are less affected by the variation in the joint typology when the total thermal resistance of the bounding layers is high ( $R_i + R_e > 2 \text{ m}^2 \text{ K/W}$ ). In these cases, the use of high-performance materials for building the joints is not needed.

The heat transfer coefficient by transmission is a key parameter in the definition of building energy performance. The analyses performed in this work demonstrate that  $H_{tr}$  can increase up to 50% when the thermal bridging effects are considered compared with an ideal insulation made of homogeneous VIP. This figure occurs with high VIP thickness, low joint thermal conductivity and low  $R_i + R_e$ . Therefore, the thermal bridging effects are significant also at the building scale.

A simple empirical model for a fast and easy evaluation of the thermal bridging effect entity was proposed. It provides results that are in good agreement with the 2D numerical analysis. The model presents some limits of applications considering that the simulations were performed considering only one VIP typology and one width of structural joint and using a limited range of VIP thicknesses. However, the range of total thermal resistance of the bounding layers and thermal resistance of structural joints cover a

significant number of realistic cases (e.g. the total thermal resistance of the bounding layers ranges from  $0.612$  to  $3.437 \text{ m}^2 \text{ K/W}$ ).

As a general guideline, the most effective ways to reduce the influence of the thermal bridges consist of increasing the total thermal resistance of the bounding layers, reducing the thermal conductivity of the VIP coupling materials and increasing the VIP size.

## REFERENCES

- Aspen Aerogels, Inc. (2015) <http://www.aerogel.com/products-and-solutions/all-insulation-products/> (accessed 21/05/2016).
- Bittner B and Lechner R (2004) *A Policy Framework for Energy Performance Assessment for Existing Dwellings*. EPA-ED Final Report. Austrian Institute for Applied Ecology, Vienna, Austria. See <http://www.ecology.at/files/berichte/E08.450-3.pdf> (accessed 21/05/2016).
- Boafo FE, Chen Z, Li C, Li B and Xu T (2014) Structure of vacuum insulation panel in building system. *Energy and Buildings* **85**: 644–653, <http://dx.doi.org/10.1016/j.enbuild.2014.06.055>.
- Boafo FE, Kim JT and Chen Z (2015) Configured cavity-core matrix for vacuum insulation panel: concept, preparation and thermophysical properties. *Energy and Buildings* **97**: 98–106, <http://dx.doi.org/10.1016/j.enbuild.2015.03.056>.
- BSI (2007a) BS EN ISO 10211:2007: Thermal bridges in building construction – heat flows and surface temperatures – detailed calculation. BSI, London, UK.
- BSI (2007b) BS EN ISO 14683:2007: Thermal bridges in building construction – linear thermal transmittance – simplified methods and default values. BSI, London, UK.
- BSI (2007c) BS EN ISO 6946:2007: Building components and building elements – thermal resistance and thermal transmittance – calculation method. BSI, London, UK.
- BSI (2008) BS EN ISO 13790:2008: Energy performance of buildings – calculation of energy use for space heating and cooling. BSI, London, UK.
- Capozzoli A, Fantucci S, Favoino F and Perino M (2015) Vacuum insulation panels: analysis of the thermal performance of both single panel and multilayer boards. *Energies* **8**: 2528–2547, <http://dx.doi.org/10.3390/en8042528>.
- Costa A, Keane MM, Torrens JI and Corry E (2013) Building operation and energy performance: monitoring, analysis and optimisation toolkit. *Applied Energy* **101**: 310–316, <http://dx.doi.org/10.1016/j.apenergy.2011.10.037>.
- Italian Ministry of Health (1975) Decreto ministeriale Sanità 5 luglio 1975, modificazioni alle istruzioni ministeriali 20 giugno 1896, relativamente all'altezza minima ed ai requisiti igienico-sanitari principali dei locali di abitazione (in Italian).
- IEA/ECBCS (International Energy Agency/Energy Conservation in Buildings and Community Systems Programme) (2001) *Vacuum Insulation in the Building Sector: Systems and Applications*, Annex 39.
- Isaia F, Fantucci S, Capozzoli A and Perino M (2015) Vacuum insulation panels: thermal bridging effects and energy



- performance in real building applications. *Energy Procedia* **83**: 269–278, <http://dx.doi.org/10.1016/j.egypro.2015.12.181>.
- Johansson P, Geving S, Hagentoft CE et al. (2014a) Interior insulation retrofit of a historical brick wall using vacuum insulation panels: hygrothermal numerical simulations and laboratory investigations. *Building and Environment* **79**: 31–45, <http://dx.doi.org/10.1016/j.buildenv.2014.04.014>.
- Johansson P, Hagentoft CE and Sasic Kalagasidis A (2014b) Retrofitting of a listed brick and wood building using vacuum insulation panels on the exterior of the facade: measurements and simulations. *Energy and Buildings* **73**: 92–104, <http://dx.doi.org/10.1016/j.enbuild.2014.01.019>.
- Kalnæs SE and Jelle BP (2014) Vacuum insulation panel products: a state-of-the-art review and future research pathways. *Applied Energy* **116**: 355–375, <http://dx.doi.org/10.1016/j.apenergy.2013.11.032>.
- Karami P, Al-Ayish N and Gudmundsson K (2015) A comparative study of the environmental impact of Swedish residential buildings with vacuum insulation panels. *Energy and Buildings* **109**: 183–194, <http://dx.doi.org/10.1016/j.enbuild.2015.10.031>.
- Lorenzati A, Fantucci S, Capozzoli A and Perino M (2014) The effect of different materials joint in vacuum insulation panels. *Energy Procedia* **62**: 374–381, <http://dx.doi.org/10.1016/j.egypro.2014.12.399>.
- Lorenzati A, Fantucci S, Capozzoli A and Perino M (2015) VIPs thermal conductivity measurement: test methods, limits and uncertainty. *Energy Procedia* **78**: 418–423, <http://dx.doi.org/10.1016/j.egypro.2015.11.686>.
- Lorenzati A, Fantucci S, Capozzoli A and Perino M (2016) Experimental and numerical investigation of thermal bridging effects of jointed vacuum insulation panels. *Energy and Buildings* **111**: 164–175, <http://dx.doi.org/10.1016/j.enbuild.2015.11.026>.
- Mandilaras I, Atsonios I, Zannis G and Founti M (2014) Thermal performance of a building envelope incorporating ETICS with vacuum insulation panels and EPS. *Energy and Buildings* **85**: 654–665, <http://dx.doi.org/10.1016/j.enbuild.2014.06.053>.
- Mukhopadhyaya P, MacLean D, Korn J, van Reenen D and Molleti S (2014) Building application and thermal performance of vacuum insulation panels (VIPs) in Canadian subarctic climate. *Energy and Buildings* **85**: 672–680, <http://dx.doi.org/10.1016/j.enbuild.2014.08.038>.
- Ogden RG, Resalati S and Kendrick CC (2013) Thermal retrofitting of existing buildings the limits of conventional technology and case for high performance vacuum technology. *Proceedings of 11th International Vacuum Insulation Symposium. Empa, Dübendorf/Zurich, Switzerland*.
- Sallée H, Quenard D, Valenti E and Galan M (2014) VIP as thermal breaker for internal insulation system. *Energy and Buildings* **85**: 631–637, <http://dx.doi.org/10.1016/j.enbuild.2014.08.039>.
- Schonhardt U, Binz A, Wohler M and Dott R (2003) *Ökobilanz eines Vakuum-Isolations-Paneels (VIP)*. Ausgearbeitet durch Institut für Energie, FHBB, Muttentz ESU-Services, Bern, Switzerland (in German).
- Simmler H and Brunner S (2005) Vacuum insulation panels for building application: basic properties, aging mechanisms and service life. *Energy and Buildings* **37**: 1122–1131, <http://dx.doi.org/10.1016/j.enbuild.2005.06.015>.
- Tenpierik MJ, van der Spoel W and Cauberg JJM (2008) Analytical models for calculating thermal bridge effects in high performance building enclosure. *Journal of Building Physics* **31(4)**: 361–387, <http://dx.doi.org/10.1177/1744259107088008>.
- UNI (Italian Organization for Standardization) (2002) UNI EN 12667:2002: Prestazione termica dei materiali e dei prodotti per edilizia – determinazione della resistenza termica con il metodo della piastra calda con anello di guardia e con il metodo del termoflussimetro – prodotti con alta e media resistenza termica. UNI, Milan, Italy (in Italian).
- UNI (2008) UNI-TS 11300-1:2008 Determinazione del fabbisogno di energia termica dell’edificio per la climatizzazione estiva ed invernale. UNI, Milan, Italy (in Italian).
- Voellinger T, Bassi A and Heitel M (2014) Facilitating the incorporation of VIP into precast concrete sandwich panels. *Energy and Buildings* **85**: 666–671, <http://dx.doi.org/10.1016/j.enbuild.2014.05.038>.
- Wakili KG, Bundi R and Binder B (2004) Effective thermal conductivity of vacuum insulation panels. *Building Research and Information* **32**: 293–299, <http://dx.doi.org/10.1080/0961321042000189644>.

#### HOW CAN YOU CONTRIBUTE?

To discuss this paper, please email up to 500 words to the editor at [journals@ice.org.uk](mailto:journals@ice.org.uk). Your contribution will be forwarded to the author(s) for a reply and, if considered appropriate by the editorial board, it will be published as discussion in a future issue of the journal.

*Proceedings* journals rely entirely on contributions from the civil engineering profession (and allied disciplines). Information about how to submit your paper online is available at [www.icevirtuallibrary.com/page/authors](http://www.icevirtuallibrary.com/page/authors), where you will also find detailed author guidelines.